Cellular Microbiology (2014) **16**(1), 50–63
doi:10.1111/cmi.12177
First published online 21 August 2013

Role of calcineurin and actin dynamics in regulated secretion of microneme proteins in *Plasmodium falciparum* merozoites during erythrocyte invasion

Shailja Singh,[†] Kunal R. More[†] and Chetan E. Chitnis*
International Centre for Genetic Engineering and Biotechnology (ICGEB), New Delhi, India.

Summary

Plasmodium falciparum **invades host erythrocytes by multiple invasion pathways. The invasion of erythrocytes by *P. falciparum* merozoites is a complex process that requires multiple interactions between host receptors and parasite ligands. A number of parasite proteins that mediate interaction with host receptors during invasion are localized to membrane-bound apical organelles referred to as micronemes and rhoptries. The timely release of these proteins to the merozoite surface is crucial for receptor engagement and invasion. It has been demonstrated previously that exposure of merozoites to a low potassium (K^+) ionic environment as found in blood plasma leads to a rise in cytosolic calcium (Ca^{2+}), which triggers microneme secretion. The signalling pathways that regulate microneme discharge in response to rise in cytosolic Ca^{2+} are not completely understood. Here, we show that a *P. falciparum* Ca^{2+}-dependent protein phosphatase, calcineurin (PfCN), is an essential regulator of Ca^{2+}-dependent microneme exocytosis. An increase in PfCN activity was observed in merozoites following exposure to a low K^+ environment. Treatment of merozoites with calcineurin inhibitors such as FK506 and cyclosporin A prior to transfer to a low K^+ environment resulted in inhibition of secretion of microneme protein apical merozoite antigen-1 (PfAMA-1). Inhibition of PfCN was shown to result in reduced dephosphorylation and depolymerization of apical actin, which appears to be critical for microneme secretion. PfCN thus serves as an effector of Ca^{2+}-dependent microneme exocytosis by regulating depolymerization of apical actin. Inhibitors that target PfCN block microneme exocytosis and limit growth of *P. falciparum* blood-stage parasites providing a novel approach towards development of new therapeutic strategies against malaria.**

Introduction

Malaria accounted for around 1.2 million deaths in 2010 (Murray *et al.*, 2012) and remains a major public health problem in the tropical world. The clinical symptoms of malaria are associated with the blood stage of the parasite life cycle during which *Plasmodium* merozoites invade and multiply within host erythrocytes. Erythrocyte invasion is a complex, multistep process which involves multiple interactions between parasite ligands and host receptors (Cowman and Crabb, 2006; Gaur and Chitnis, 2011). A number of parasite ligands involved in these interactions are localized in apical organelles of *Plasmodium* merozoites that are referred to as micronemes and rhoptries (Cowman and Crabb, 2006; Gaur and Chitnis, 2011). The timely discharge of these proteins to the merozoite surface is crucial for receptor engagement during the process of invasion.

Cytosolic calcium (Ca^{2+}) plays an important role as a second messenger to regulate microneme secretion in *Plasmodium falciparum* and the related apicomplexan *Toxoplasma gondii* (Carruthers *et al.*, 1999; Carruthers and Sibley, 1999; Lovett *et al.*, 2002; Singh *et al.*, 2010). Increase in cytosolic Ca^{2+} following treatment of *P. falciparum* merozoites and *T. gondii* tachyzoites with the ionophore A23187 has been shown to trigger microneme discharge (Carruthers and Sibley, 1999; Lovett *et al.*, 2002; Singh *et al.*, 2010). Several molecules have been shown to participate as effectors in Ca^{2+}-dependent discharge of microneme proteins. Ca^{2+}-binding c2 domain containing proteins, PfDOC2.1 and TgDOC2.1, which are localized on the microneme surface, mediate microneme discharge in *P. falciparum* and *T. gondii* respectively (Farrell *et al.*, 2012). Ca^{2+}-dependent protein kinases, PfCDPK1 and TgCDPK1, have also been

Received 14 March, 2013; revised 16 July, 2013; accepted 30 July, 2013. *For correspondence. E-mail cchitnis@icgeb.res.in; Tel. (+91) 11 2674 1358l; Fax (+91) 11 2674 2316.
[†]Kunal R. More and Shailja Singh have contributed equally to the work.

implicated in microneme secretion (Lourido *et al*., 2010; Bansal *et al*., 2013). Several phosphorylation and dephosphorylation events involving different kinases and phosphatases, respectively, mediate Ca^{2+}-dependent signal transduction pathways leading to regulated secretion of vesicles in many mammalian cell types (Lang, 1999; Grybko *et al*., 2007). These studies revealed that the Ca^{2+}-dependent phosphatase calcineurin (CN) plays a central role in regulated vesicle exocytosis in mammalian cells (Grybko *et al*., 2007; Pores-Fernando *et al*., 2009). CN is also involved in regulation of exocytosis and membrane fusion in *Paramecium tetraurelia* (Momayezi *et al*., 1987) and in the dephosphorylation of cytoskeletal components such as myosin, tubulin and actin (Goto *et al*., 1985; Li and Handschumacher, 2002; Silverman-Gavrila and Charlton, 2009).

CN, a serine- and threonine-specific protein phosphatase that is expressed in all eukaryotes, senses Ca^{2+} through its activation by calmodulin (Klee *et al*., 1979). CN is a heterodimer containing a catalytic/calmodulin-binding subunit, CNA, which is tightly bound to a Ca^{2+}-binding regulatory subunit, CNB (Hemenway and Heitman, 1999). It has been known for over a decade that the immunosuppressive drugs FK506 and CsA, when bound to proteins called FK506-binding proteins (FKBPs) and cyclophilins, respectively, act as potent, specific inhibitors of CN activity (Liu *et al*., 1991; O'Keefe *et al*., 1992; Swanson *et al*., 1992; Mukai *et al*., 1993; Schreiber and Crabtree, 1993; Wiederrecht *et al*., 1993; Griffith *et al*., 1995; Ho *et al*., 1996; Huai *et al*., 2002).

The catalytic, calmodulin-binding subunit of *P. falciparum* CN (PfCN), PfCNA (encoded by PF3D7_0802800), and the Ca^{2+}-binding regulatory subunit, PfCNB (encoded by PF3D7_1451700), are expressed in *P. falciparum* blood-stage parasites (http://plasmodb.org; Dobson *et al*., 1999; Kumar *et al*., 2004; Kumar *et al*., 2005). CsA and FK506 have been shown to inhibit PfCN activity and block blood-stage parasite growth (Thommen-Scott, 1981; Nickell *et al*., 1982; Kumar *et al*., 2004; 2005). In this study we investigate the role of PfCN in Ca^{2+}-dependent microneme exocytosis, an essential step in erythrocyte invasion by *Plasmodium* merozoites. We demonstrate that treatment of *P. falciparum* merozoites with PfCN inhibitors CsA and FK506 results in reduced secretion of microneme proteins such as apical membrane antigen-1 (PfAMA1). We also demonstrate that treatment of merozoites with PfCN inhibitors results in reduced depolymerization of apical cortical actin resulting in vesicle secretion. These results reveal that PfCN serves as an effector of Ca^{2+}-dependent microneme exocytosis by regulating depolymerization of apical cortical actin. Given its central role in microneme exocytosis, PfCN may serve as a potent target for inhibition of erythrocyte invasion by *P. falciparum* merozoites for the treatment of malaria.

Results

CN activity in P. falciparum *merozoites exposed to an extracellular-like ionic environment*

We have previously demonstrated that exposure of *P. falciparum* merozoites to an extracellular-like ionic environment as found in blood plasma (EC buffer – 140 mM NaCl, 5 mM KCl, 1 mM $CaCl_2$) leads to a rise in cytosolic Ca^{2+} levels, which triggers microneme secretion (Singh *et al*., 2010). Such a rise in cytosolic Ca^{2+} can activate the Ca^{2+}-dependent phosphatase, PfCN. We therefore measured CN activity in *P. falciparum* merozoites following transfer from a buffer mimicking intracellular ionic environment (IC buffer – 5 mM NaCl, 140 mM KCl, 1 mM EGTA) to EC buffer (Fig. 1A) using a CN activity assay. The assay uses phosphopeptide RII, which is a known peptide substrate of CN (Donella-Deana *et al*., 1994; Enz *et al*., 1994). The detection of released free phosphate is based on the classic Malachite green assay using BIOMOL GREEN reagent (Martin *et al*., 1985). This assay is used routinely for assessment of CN activity and effect of CN inhibitors in both mammalian and protozoan systems (Dobson *et al*., 1999; Carrero *et al*., 2004; Su *et al*., 2012; Karch *et al*., 2013).

An increase in PfCN activity was observed in merozoites following transfer from IC buffer to EC buffer indicating that exposure to extracellular-like ionic environment triggers a rise in PfCN activity in *P. falciparum* merozoites (Fig. 1A). This increase in CN activity was inhibited when *P. falciparum* merozoites isolated in IC buffer were treated with CN inhibitors FK506 (5 μM) and CsA (25 μM) for 15 min prior to transfer to EC. Both FK506 and CsA did not have any effect on the rise of cytosolic Ca^{2+} in merozoites (Fig. 1B) suggesting that they directly inhibit PfCN activity.

PfCN activity is required for microneme secretion and erythrocyte invasion of P. falciparum *merozoites*

To test whether PfCN activity is required for the release of microneme proteins, we studied the secretion of microneme proteins EBA-175 and PfAMA-1 from *P. falciparum* merozoites following transfer to EC buffer with and without prior treatment with CN inhibitors FK506 and CsA (Fig. 1C). Transfer of merozoites from IC buffer to EC buffer triggers secretion of EBA175 and PfAMA-1 (Fig. 1C) as reported previously (Singh *et al*., 2010). Treatment of merozoites with CN inhibitors prior to transfer from IC to EC buffer inhibits secretion of both EBA-175

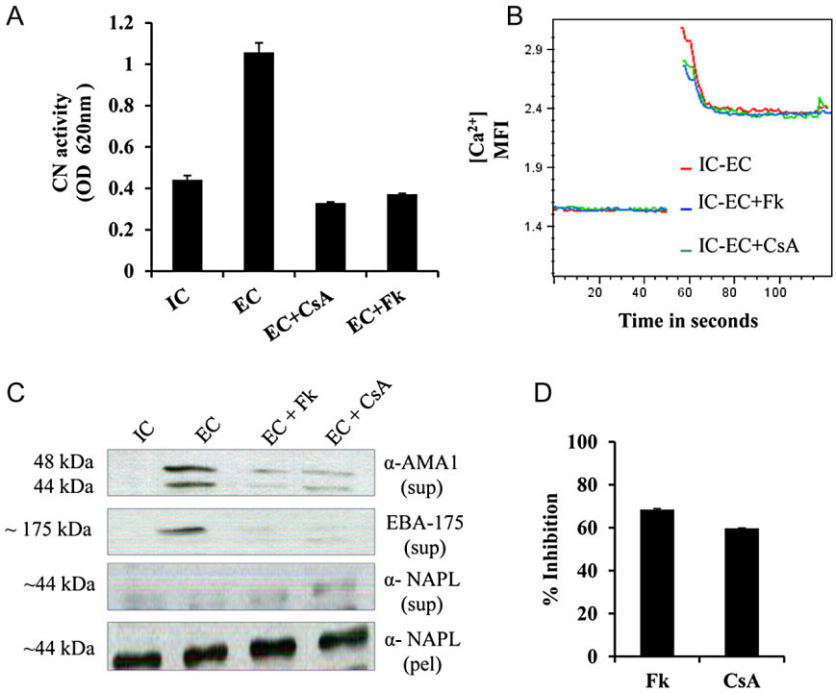

Fig. 1. CN activity in *P. falciparum* merozoites and its role in microneme secretion.
A. *In vivo* CN activity in merozoites under different ionic conditions. Activity of PfCN was assessed in *P. falciparum* merozoites using calcineurin cellular activity assay kit (Enzo life sciences). *P. falciparum* merozoites isolated in buffer mimicking intracellular ionic conditions (IC buffer – 5 mM NaCl, 140 mM KCl, 1 mM EGTA), were transferred to buffer mimicking extracellular ionic conditions (EC buffer – 140 mM NaCl, 5 mM KCl, 1 mM $CaCl_2$) with or without treatment with CN inhibitors FK506 (EC + Fk) or CsA (EC + CsA). Transfer of merozoites from IC to EC buffer triggers PfCN activity. Treatment of merozoites with CN inhibitors FK506 and CsA reduces PfCN activity. Error bars represent standard deviation from three independent experiments.
B. Changes in cytosolic calcium levels in *P. falciparum* 3D7 merozoites following transfer from IC to EC buffer and on addition of CN inhibitors. *P. falciparum* merozoites isolated in IC buffer were labelled with Fluo-4AM and cytosolic calcium [Ca^{2+}] levels were measured by flow cytometry before and after transfer from IC to EC buffer (IC-EC) or to EC buffer containing FK506 (IC-EC + Fk) or CsA (IC-EC + CsA). Treatment with CN inhibitors does not affect rise in cytosolic Ca^{2+} in merozoites following transfer from IC to EC buffer.
C. Inhibition of microneme discharge by CN inhibitors. *P. falciparum* merozoites isolated in IC buffer were transferred to EC buffer either with or without treatment with CN inhibitors FK506 or CsA. Discharge of microneme proteins PfAMA1 and PfEBA-175 was detected in merozoite supernatants by Western blotting using specific antisera. Merozoite supernatants and pellets were also probed with antisera raised against cytoplasmic protein PfNAPL to detect merozoite lysis and confirm that similar numbers of merozoites were used under different conditions respectively. Treatment of merozoites with CN inhibitors during transfer from IC to EC buffer inhibits discharge of microneme proteins.
D. CN inhibitors block erythrocyte invasion by *P. falciparum* merozoites. *P. falciparum* merozoites isolated in IC buffer were added to erythrocytes resuspended in RPMI with or without CN inhibitors FK506 (5 μM) and CsA (25 μM) to allow invasion. Newly invaded rings were scored by Giemsa staining 24–26 h post invasion. Per cent (%) inhibition of invasion with different CN inhibitors compared with invasion in absence of inhibitors is shown. Error bars represent standard deviation from three independent experiments. Treatment of merozoites with CN inhibitors blocks erythrocyte invasion by *P. falciparum* merozoites.

and PfAMA-1 (Fig. 1C) suggesting that PfCN plays an important functional role in regulated exocytosis of microneme proteins.

Discharge of micronemes is an essential step in erythrocyte invasion by *P. falciparum* merozoites (Cowman and Crabb, 2006; Gaur and Chitnis, 2011). In order to test if inhibition of PfCN can block erythrocyte invasion, *P. falciparum* merozoites isolated in IC buffer were treated with FK506 and CsA and transferred to complete RPMI medium containing erythrocytes to allow invasion. Newly invaded ring-stage parasites were scored by Giemsa staining. Treatment of merozoites with FK506 and CsA reduced the efficiency of erythrocyte invasion (Fig. 1D).

Changes in phosphorylation of P. falciparum *merozoite proteins following treatment with PfCN inhibitors*

The observation that inhibition of PfCN activity results in inhibition of microneme secretion suggests that dephosphorylation of target merozoite proteins by PfCN may regulate microneme secretion. We compared levels of protein phosphorylation in *P. falciparum* merozoites in IC buffer and following transfer to EC buffer with or without pre-treatment with CN inhibitors FK506 and CsA. Changes in phosphorylation levels of merozoite proteins were detected by staining merozoite lysates separated by SDS-PAGE with Pro-Q Diamond, which stains

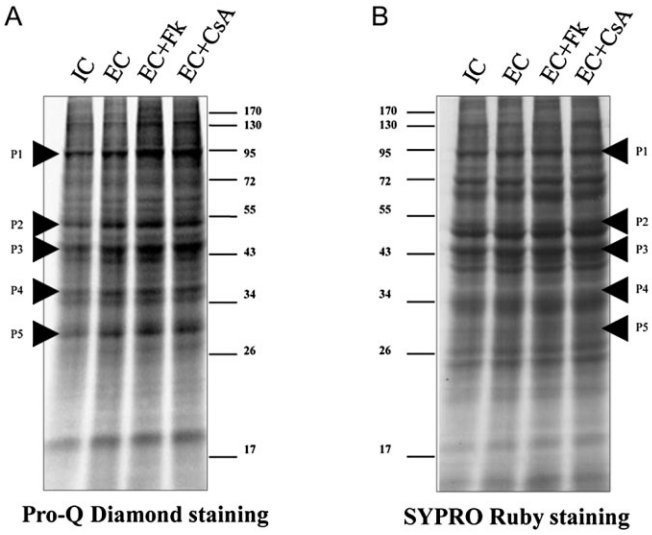

C

Band number	EC/IC	EC+Fk/IC	EC+CsA/IC	Identified Proteins
P1	1.26	1.44	1.50	Heat Shock Protein-90
P2	1.32	1.53	1.55	Phosphoglycerate kinase
P3	1.30	1.60	1.60	Actin-1
P4	1.30	1.47	1.60	Adenosine deaminase
P5	1.25	1.60	1.90	Glyceraldehyde-3-phosphate dehydrogenase

Fig. 2. Inhibition of CN activity modulates protein phosphorylation in *P. falciparum* merozoites. *P. falciparum* merozoites isolated in buffer mimicking intracellular ionic conditions (IC – 5 mM NaCl, 140 mM KCl, 1 mM EGTA) were transferred to buffer mimicking extracellular ionic conditions (EC – 140 mM NaCl, 5 mM KCl, 1 mM $CaCl_2$) with or without treatment with CN inhibitors FK506 (EC + Fk) and cyclosporin A (EC + CsA). Lysates of merozoites under these conditions were separated by SDS-PAGE and phosphorylated proteins were detected by Pro-Q Diamond staining (A). After washing out Pro-Q Diamond, the same gel was stained with SYPRO Ruby to detect total proteins (B). The fluorescence intensities of Pro-Q Diamond and SYPRO Ruby stained gels were recorded with a Typhoon Phosphoimager. Arrowheads indicate protein bands (P1 to P5) whose phosphorylation appears to increase from IC to EC with further increase upon treatment with CN inhibitors FK506 and CsA. The ratio of phosphorylation signal intensity normalized for total protein in bands P1 to P5 for different conditions is shown in the table (C). The identity of proteins present in bands P1 to P5 as identified by mass spectrometry are also shown in the table (C).

phospho-proteins (Schulenberg *et al*., 2003) (Fig. 2A). Phosphorylation levels of proteins were quantified by densitometry analysis of Pro-Q Diamond stained SDS-PAGE gels. Total amounts of individual proteins were quantified by densitometry analysis of SDS-PAGE gels stained with SYPRO Ruby and used for normalization of fold increase in protein phosphorylation as determined by Pro-Q Diamond staining (Fig. 2B). Five protein bands (P1 to P5) showed significant fold increase (> 1.2-fold) in phosphorylation in EC buffer compared with IC buffer (Fig. 2). Treatment with FK506 or CsA prior to transfer to EC buffer resulted in further increase (> 1.4-fold) in phosphorylation signal for each of these protein bands (Fig. 2C). The identity of proteins in bands P1 to P5 was determined by mass spectrometry in two independent experiments. For each band, the protein matches identified by Mascot search with scores above significance are listed in Supplementary Table S1. Proteins that were identified in bands P1 to P5 in both experiments and that had the highest cumulative scores are listed in Fig. 2C. Of the proteins identified, actin, which was detected in band P3 was selected for further analysis as its role in vesicle secretion in mammalian cells is well established (Muallem *et al*., 1995; Yoneda *et al*., 2000).

Phosphorylation status of actin under different environmental conditions was confirmed by radiolabelling using [γ-^{32}P]-ATP followed by immunoprecipitation using anti-actin rabbit sera. *P. falciparum* merozoites were isolated in IC buffer and transferred to EC buffer with or without treatment with CN inhibitors FK506 and CsA in presence of [γ-^{32}P]-ATP to allow radiolabelling of phosphorylated proteins. Lysates of merozoites under these different conditions were used for immunoprecipitation using anti-actin rabbit sera. Phosphorylated actin was detected by autoradiography. Transfer of merozoites to EC buffer led to phosphorylation of actin and phosphorylation levels increased if merozoites were treated with CN inhibitors (Fig. 3). These observations suggest that actin is a dephosphorylation substrate for PfCN.

Changes in polymerization status of actin in P. falciparum *merozoites following changes in ionic environment and treatment with PfCN inhibitors*

Phosphorylation of actin has been shown to regulate the polymerization state of actin (Ohta *et al*., 1987; Baba *et al*., 2003). Moreover, depolymerization of actin under the plasma membrane surface is necessary for vesicular

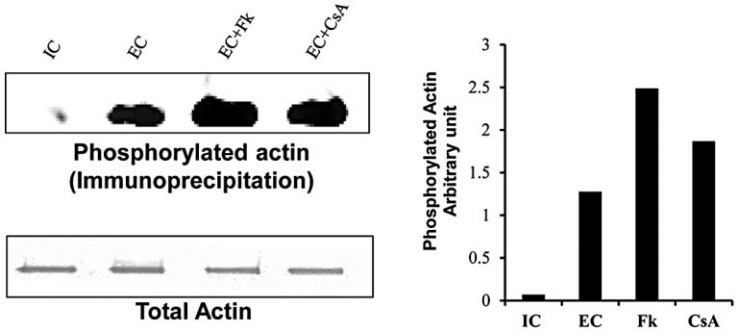

Fig. 3. Inhibition of actin phosphorylation by treatment of *P. falciparum* merozoites with CN inhibitors. *P. falciparum* merozoites isolated in buffer mimicking intracellular ionic conditions (IC – 5 mM NaCl, 140 mM KCl, 1 mM EGTA) were transferred and incubated for 5 min in buffer mimicking extracellular ionic conditions (EC – 140 mM NaCl, 5 mM KCl, 1 mM $CaCl_2$) containing [γ-^{32}P]-ATP with or without treatment with CN inhibitors FK506 (EC + Fk) and cyclosporin A (EC + CsA). Actin was immunoprecipitated from merozoite lysates, separated on SDS-PAGE gel and analysed by autoradiography to detect phosphorylation with ^{32}P. Total actin immunoprecipitated under different conditions was determined by Western blotting using anti-actin rabbit sera. Actin is phosphorylated upon transfer to EC buffer and level of phosphorylation is higher in presence of CN inhibitors. Actin thus appears to be a dephosphorylation substrate for PfCN.

exocytosis in mammalian cells (Vitale *et al*., 1991; Tobin *et al*., 2012). We examined the polymerization status of actin in *P. falciparum* merozoites exposed to different ionic environments and following treatment with PfCN inhibitors. *P. falciparum* merozoites were isolated in IC buffer and transferred to EC buffer either with or without treatment with FK506 and CsA. Merozoites lysates were prepared under each condition and polymerized/depolymerized actin were separated by ultracentrifugation as described previously (Tu *et al*., 2003). Both the ultracentrifugation pellet containing polymerized actin (or F-actin) and supernatant containing depolymerized actin (or G-actin) were separated on SDS-PAGE gel, transferred to nitrocellulose and probed by Western blotting using anti-actin rabbit sera. Lysates made from merozoites incubated in IC buffer contained higher amounts of polymerized actin (ICp) than depolymerized actin (ICs) whereas lysates from merozoites in EC buffer had more depolymerized actin (ECs) compared with polymerized actin (ECp) (Fig. 4). Treatment of merozoites with PfCN inhibitors FK506 or CsA resulted in increase in polymerized actin (Fig. 4). Actin polymerization status was also determined in merozoites in EC buffer treated with actin depolymerizing agent cytochalasin D (CytD) and polymerized actin stabilizing agent jasplakinolide (JAS) as controls. Treatment of merozoites with JAS resulted in increase in polymerized actin levels (Fig. 4) while treatment with CytD resulted in reduced levels of polymerized actin (Fig. 4). These results together demonstrate that activation of PfCN results in depolymerization of actin in *P. falciparum* merozoites.

Phalloidin and its fluorescent derivatives have been shown to bind *P. falciparum* F-actin (Webb *et al*., 1996). Here we have used Alexa 488-labelled phalloidin in immunofluorescence assays (IFA) to visualize the distribution of F-actin in *P. falciparum* merozoites under different conditions (Fig. 5). Antibodies against EBA175 were used to define the location of micronemes at the apical end by IFA. F-actin is primarily localized at the apical end of merozoites in IC buffer (Fig. 5A). The amount of F-actin as detected by phalloidin staining decreases in merozoites in EC buffer (Fig. 5B). Treatment of merozoites with CN inhibitors FK506 or CsA results in accumulation of polymerized F-actin at the apical end of *P. falciparum*

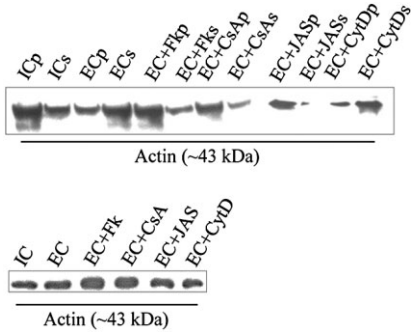

	Ratio P/S
IC	1.60
EC	0.50
Fk	2.80
CsA	4.27
JAS	14.70
CytD	0.27

Fig. 4. Polymerization status of actin in *P. falciparum* merozoites under different environmental conditions and in presence of CN inhibitors and actin modulators. *P. falciparum* merozoites isolated in buffer mimicking intracellular ionic conditions (IC buffer – 5 mM NaCl, 140 mM KCl, 1 mM EGTA), were transferred to buffer mimicking extracellular ionic conditions (EC buffer – 140 mM NaCl, 5 mM KCl, 1 mM $CaCl_2$) with or without treatment with CN inhibitors FK506 (EC + Fk) and cyclosporin A (EC + CsA) or actin modulators, cytochalasin D (CytD) and jasplakinolide (JAS). Lysates of merozoites in different conditions were separated by SDS-PAGE and levels of total actin were determined by Western blotting using anti-actin rabbit sera. Levels of polymerized F-actin and monomeric G-actin in merozoites were determined by ultracentrifugation of merozoite lysates and detection of actin in pellet (p) and supernatant (s), respectively, by Western blotting using anti-actin rabbit sera. Densitometry scanning of the Western blots was used to determine the ratio of polymerized F-actin (P) to monomeric G-actin (S) in merozoites under different conditions. Ratios of polymerized and monomeric actin (P/S) detected in merozoites under different conditions are shown.

merozoites (Fig. 5C and D). Treatment of *P. falciparum* merozoites with CytD results in reduced levels of F-actin whereas treatment with JAS leads to accumulation of F-actin at the apical end (Fig. 5E and F). Rabbit sera raised against actin, which recognize both polymerized and monomeric actin, confirm that the total amount of actin in merozoites remains unchanged in different conditions (Fig. 5A–F and Supplementary Fig. S1).

Polymerization status of actin regulates microneme secretion in P. falciparum *merozoites*

Our results demonstrate that exposure of *P. falciparum* merozoites to low K^+ environment leads to increase in cytosolic Ca^{2+}, which activates PfCN and leads to microneme discharge. In addition, we found that activation of PfCN leads to dephosphorylation and depolymerization of actin. To understand whether depolymerization of actin has any role in Ca^{2+}-regulated secretion of microneme proteins, we tested the effect of several modulators of actin polymerization on microneme discharge. These modulators included cytochalasin D (CytD) and mycalolide B (ML-B), which inhibit actin polymerization, latrunculin B (LA-B), which depolymerizes F-actin, and jasplakinolide (JAS), which stabilizes polymerized actin. Treatment of merozoites with actin depolymerizing agents, CytD, ML-B and LA-B, resulted in increased secretion of microneme protein PfAMA-1 (Fig. 6A–C) whereas treatment with polymerized actin stabilizer JAS resulted in reduced secretion of PfAMA-1 (Fig. 6D). Merozoite supernatants and pellets were also probed with antisera raised against cytoplasmic protein PfNAPL to control for merozoite lysis and confirm that similar numbers of merozoites were used for different conditions respectively. These results indicate that actin depolymerization promotes microneme secretion in *P. falciparum* merozoites. None of the actin modulating agents that were tested inhibit PfCN activity (Supplementary Fig. S2). Actin modulators such as JAS that increase levels of polymerized actin inhibit erythrocyte invasion by *P. falciparum* merozoites (Supplementary Fig. S3).

Discussion

The invasive stages of *Plasmodium* and *Toxoplasma* possess secretory organelles at the apical end referred to as micronemes and rhoptries that contain protein ligands capable of binding target receptors to mediate invasion of host cells (Carruthers *et al*., 1999; Carruthers and Sibley, 1999; Lovett *et al*., 2002; Singh *et al*., 2010). The timely secretion of microneme and rhoptry proteins to the parasite surface is essential for receptor engagement, a key step in the invasion process. We have previously demonstrated that exposure of *P. falciparum* merozoites to a low K^+ environment as found in blood plasma results in a rise in cytosolic Ca^{2+}, which triggers release of microneme proteins such as EBA175 and PfAMA1 to the merozoite surface (Singh *et al*., 2010; Bansal *et al*., 2013). Subsequently, the binding of EBA175 and its homologues with their receptors on host erythrocytes restores basal cytosolic Ca^{2+} levels and triggers the release of rhoptry proteins such as PfRH2 and PfTRAMP (Singh *et al*., 2010; Siddiqui *et al*., 2013), which also bind erythrocyte receptors for invasion. The sequential release of microneme and rhoptry proteins thus enables a cascade of receptor-ligand interactions that mediate the invasion process.

Ca^{2+} has been shown to serve as a second messenger to regulate vesicle secretion in diverse eukaryotic cells (Lang, 1999). A number of Ca^{2+}-dependent effectors that mediate vesicle secretion in response to rise in cytosolic Ca^{2+} levels have been identified (Lang, 1999; Grybko *et al*., 2007; Pores-Fernando *et al*., 2009). Ca^{2+}-dependent protein kinase-1 (CDPK1) is involved in regulating microneme secretion in *T. gondii* as well as *P. falciparum* (Lourido *et al*., 2010; Bansal *et al*., 2013) indicating that protein phosphorylation plays a central role in this process. The Ca^{2+}-dependent phosphatase, calcineurin (CN), is also implicated in regulation of vesicle secretion in response to changes in cytosolic Ca^{2+} levels in diverse eukaryotic cells (Goto *et al*., 1985; Grybko *et al*., 2007; Pores-Fernando *et al*., 2009). RNA expression studies show that orthologues of catalytic subunit CNA and regulatory subunit CNB are expressed in late blood stages of *P. falciparum* (http://plasmodb.org). Moreover, PfCN is essential for growth of *P. falciparum* blood stages (Thommen-Scott, 1981; Kumar *et al*., 2004; 2005). A recent report also confirms the expression of both PfCN subunits in *P. falciparum* late stages through mass spectrometric analysis (Treeck *et al*., 2011). Here, we have explored the potential role of PfCN in microneme exocytosis in *P. falciparum* merozoites.

Transfer of *P. falciparum* merozoites from IC buffer to EC buffer resulted in an increase in PfCN activity which is inhibited by pre-treatment with CN inhibitors FK506 and CsA. CsA has been shown to specifically inhibit phosphatase activity of recombinant PfCN previously (Dobson *et al*., 1999). Pre-treatment of *P. falciparum* merozoites with CsA and FK506 also resulted in reduced secretion of microneme proteins PfAMA1 and EBA-175. The observation that two distinct CN inhibitors block microneme secretion suggests that PfCN plays a critical role in regulating microneme secretion.

Next, we attempted to identify the parasite proteins whose phosphorylation status changes in response to activation of PfCN. The five proteins identified whose phosphorylation status changes when *P. falciparum*

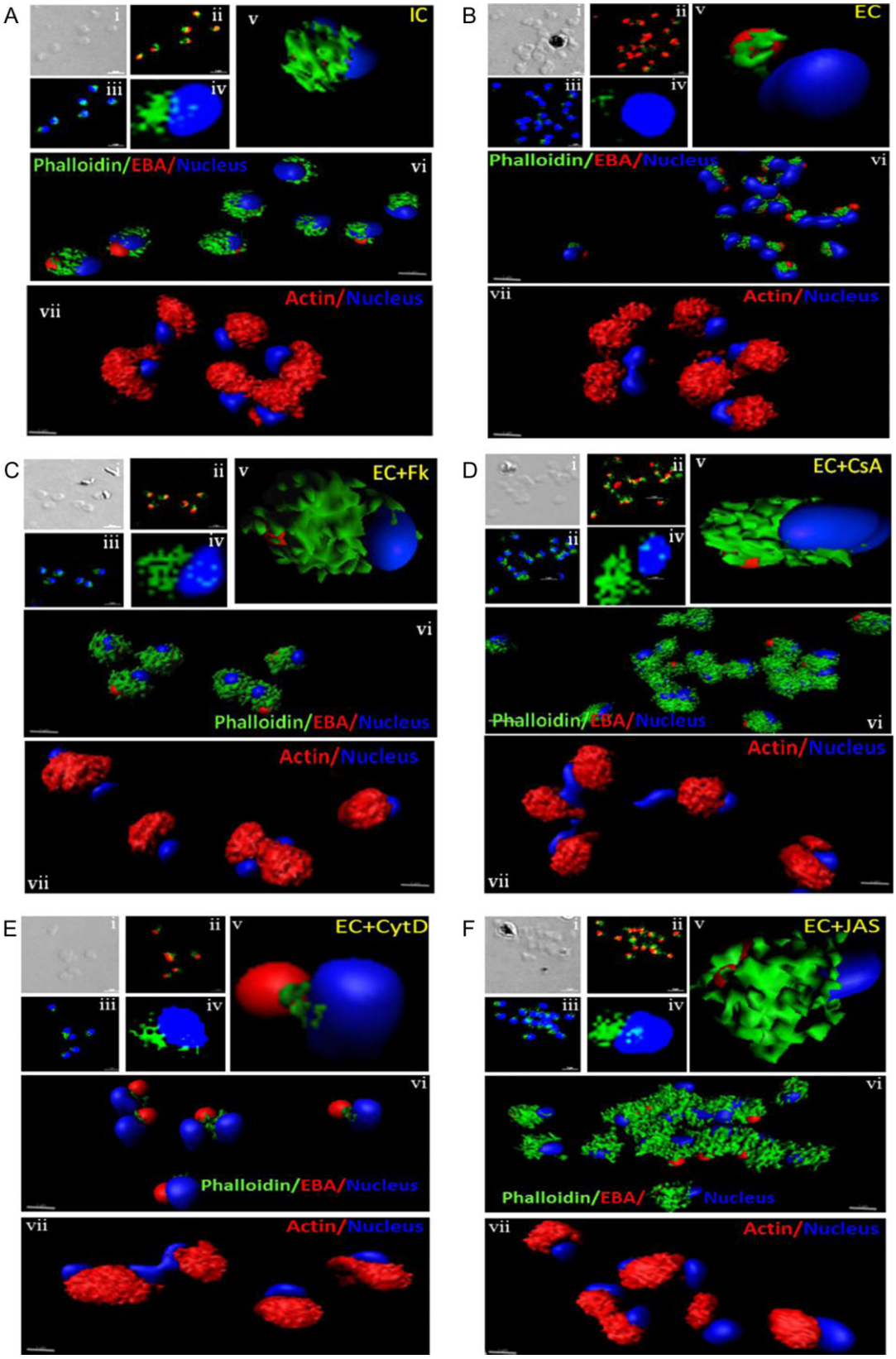
A
i
ii
iii
iv
v
IC
Phalloidin/EBA/Nucleus
vi
vii
Actin/Nucleus
B
EC
C
EC+Fk
D
EC+CsA
E
EC+CytD
F
EC+JAS

Fig. 5. Actin polymerization status in *P. falciparum* merozoites. *P. falciparum* merozoites isolated in buffer mimicking intracellular ionic conditions (IC buffer – 5 mM NaCl, 140 mM KCl, 1 mM EGTA) (A) were transferred to buffer mimicking extracellular ionic conditions (EC buffer – 140 mM NaCl, 5 mM KCl, 1 mM $CaCl_2$) (B) or EC buffer with CN inhibitors, FK506 (C) and cyclosporin A (CsA) (D), or Ec buffer with actin modulators, cytochalasin D (CytD) (E) and jasplakinolide (JAS) (F). Merozoites were stained with Alexa 488-labelled phalloidin to detect polymerized F-actin (green), mouse anti-EBA-175 mouse sera and Alexa Fluor 594-conjugated anti-mouse IgG goat antibodies to define location of micronemes (red) and DAPI to define location of nuclei (blue). Slides were observed under a confocal laser microscope (Nikon A1R). Bright-field (i) and single slice confocal fluorescence images of merozoites (ii–iv) are shown. Three-dimensional reconstruction of confocal z stack fluorescence images of merozoites was performed using Imaris software (v–vii). Total actin (polymerized F-actin and monomeric G-actin) was detected with anti-actin rabbit sera followed by Alexa Fluor 594-conjugated anti-rabbit IgG goat antibodies (red in vii). Levels of total actin are similar in all conditions tested. Transfer of merozoites from IC to EC buffer leads to disassembly of polymerized F-actin at the apical tip of merozoites. Treatment of merozoites with FK506 and CsA prior to transfer to EC buffer leads to accumulation of polymerized actin at the apical end. Actin depolymerizing agent CytD and actin stabilizing agent JAS were used as control and result in reduced F-actin and increased F-actin at the apical tip of the merozoites respectively. Scale bar represents 1 μm.

merozoites are shifted from IC buffer to EC buffer and following treatment with CN inhibitors FK506 and CsA includes actin, which has been previously shown to play a role in vesicle secretion (Aunis and Bader, 1988; Yoneda *et al*., 2000) (Fig. 2). Radiolabelling of merozoites with [γ-^{32}P]-ATP following transfer from IC to EC buffer in presence of CN inhibitors and detection of phosphorylated actin by immunoprecipitation confirmed that actin serves as a dephosphorylation substrate for PfCN in response to a rise in cytosolic Ca^{2+}.

The phosphorylation of actin is reported to regulate its polymerization status (Ohta *et al*., 1987; Baba *et al*., 2003). We investigated the polymerization status of actin in *P. falciparum* merozoites in IC buffer and after transfer

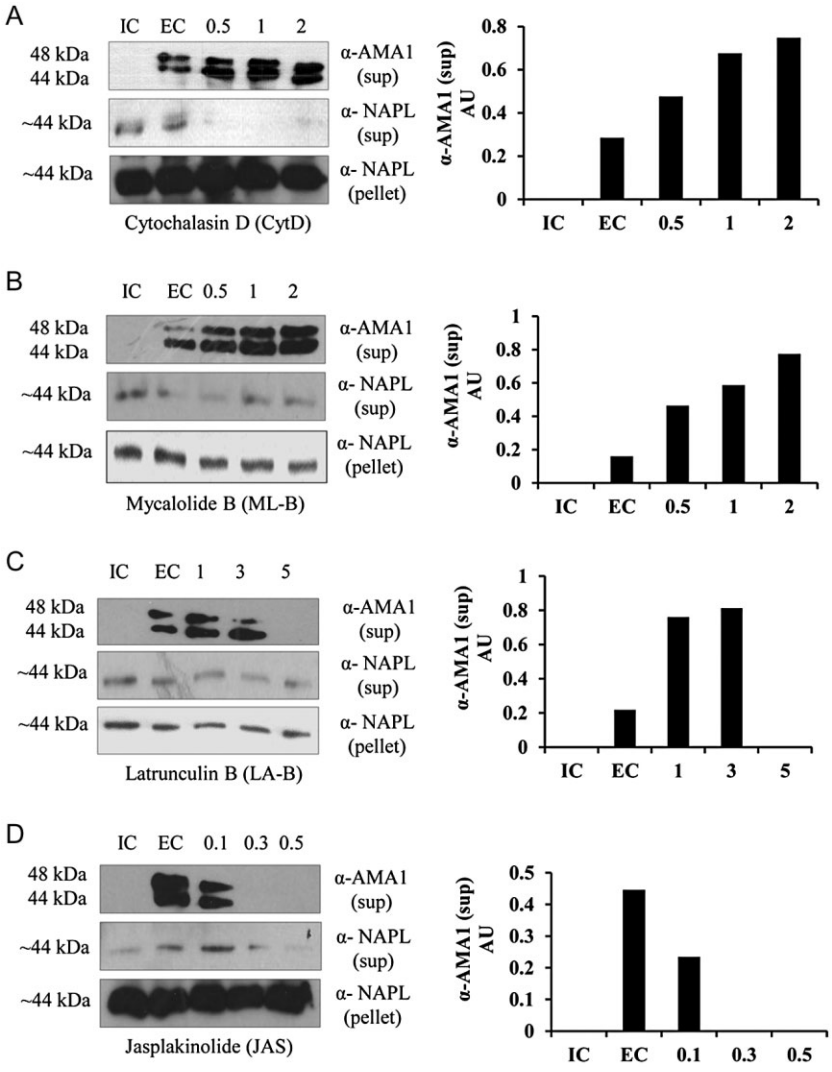

Fig. 6. Depolymerization of actin results in increased microneme secretion. *P. falciparum* merozoites isolated in buffer mimicking intracellular ionic conditions (IC buffer – 5 mM NaCl, 140 mM KCl, 1 mM EGTA) were transferred to buffer mimicking extracellular ionic conditions (EC buffer – 140 mM NaCl, 5 mM KCl, 1 mM $CaCl_2$) in presence of different concentrations of actin modulators including cytochalasin D (CytD) (A), mycalolide B (ML-B) (B), latrunculin B (LA-B) (C) or jasplakinolide (JAS) (D). Concentrations of actin modulators used are shown in μM. Secretion of microneme protein PfAMA1 was detected in merozoite supernatants by Western blotting. Merozoite supernatants and pellets were also probed with antisera raised against cytoplasmic protein PfNAPL to detect merozoite lysis (NAPL sup) and confirm that similar numbers of merozoites were used (NAPL pellet) respectively. Transfer of merozoites from IC to EC buffer leads to discharge of PfAMA1. Treatment of merozoites with actin depolymerizing agents CytD, LA-B and ML-B increases microneme discharge in a dose-dependent manner. Microneme discharge is blocked at highest concentration of LA-B used. Polymerized actin stabilizing agent JAS results in reduced microneme discharge. Graphs indicate relative amounts of PfAMA1 secreted in supernatant as measured by ImageJ after normalization with NAPL (pellet) and NAPL (sup) data. AU, arbitrary unit.

to EC buffer either with or without treatment with PfCN inhibitors FK506 and CsA. Fractions containing F-actin polymers and G-actin monomers were separated by ultracentrifugation of merozoite lysates as described previously (Tu *et al*., 2003; Schmitz *et al*., 2010). Western blotting with rabbit sera against actin revealed that the amount of F-actin, which separates in the pellet fraction, decreases following transfer of merozoites from IC buffer to EC buffer. Pre-treatment of merozoites with CN inhibitors FK506 and CsA prior to transfer to EC buffer leads to accumulation of F-actin. In parallel control experiments, CytD treatment led to decrease in F-actin and JAS treatment resulted in increase in F-actin levels in *P. falciparum* merozoite lysates (Fig. 4). These results were consistent with our findings based on staining for F-actin with Alexa 488-phalloidin in *P. falciparum* merozoites. Alexa 488-phalloidin staining indicates that F-actin is primarily localized at the apical end of *P. falciparum* merozoites. The fluorescence signal from Alexa 488-phalloidin decreases following transfer of merozoites to EC buffer suggesting that the F-actin network under the plasma membrane at the apical end of the merozoites is disassembled. This decrease in Alexa 488-phalloidin signal is inhibited if merozoites are treated with FK506 or CsA prior to transfer to EC buffer (Fig. 5). These results suggest that activation of PfCN following transfer of merozoites to EC buffer leads to dephosphorylation and depolymerization of F-actin at the apical end of *P. falciparum* merozoites.

The dynamics of actin depolymerization plays a key role in regulation of vesicle secretion (Aunis and Bader, 1988; Muallem *et al*., 1995; Yoneda *et al*., 2000; Eitzen, 2003). Depolymerization of F-actin has been shown to promote vesicle fusion and secretion in mammalian cells (Vitale *et al*., 1991). Here, we have tested the potential role of actin depolymerization in microneme secretion by *P. falciparum* merozoites. *P. falciparum* merozoites were transferred from IC buffer to EC buffer in presence of CytD, ML-B or LA-B, which directly target actin by capping the barbed ends of filaments, promoting F-actin severing and sequestering actin monomers, respectively, to prevent polymerization of actin filaments. Alternatively, merozoites were pre-treated with JAS, which stabilizes F-actin filaments to promote actin polymerization (Saito *et al*., 1994; Spector *et al*., 1999; Johns *et al*., 2001; Eitzen, 2003). While CytD and ML-B treatment led to increase in secretion of microneme protein PfAMA1, treatment with JAS reduced PfAMA1 secretion. Interestingly, LA-B treatment increased microneme secretion when used at low concentrations but inhibited secretion at higher concentrations (Fig. 6C). The inhibition observed at high LA-B concentrations may be due to complete sequestration of monomeric actin demonstrating that minimal F-actin structures may be required for microneme secretion. A similar biphasic effect on the secretory activity of chromaffin cells was reported previously with low doses of LA-B enhancing exocytosis but higher concentrations inhibiting vesicle secretion (Johns *et al*., 2001; Gasman *et al*., 2004). These results confirm that depolymerization of F-actin promotes microneme exocytosis suggesting that the cortical F-actin network may present a 'physical barrier' at the plasma membrane that prevents vesicle fusion and exocytosis. In conclusion, the activation of PfCN following exposure of *P. falciparum* merozoites to an extracellular-like ionic environment with low K^+ results in the dephosphorylation and depolymerization of F-actin at the apical end enabling the fusion of micronemes with the merozoite plasma membrane leading to the secretion of microneme proteins such as PfAMA1 and EBA175 (Fig. 7). PfCN thus plays a key role in regulation of microneme secretion and provides a promising target for the development of inhibitors that block invasion and limit parasite growth.

Experimental procedures

Culture of P. falciparum *3D7 strain and isolation of viable merozoites*

Cryopreserved *P. falciparum* 3D7 was cultured in O^{+ve} erythrocytes at 5% haematocrit in RPMI 1640 medium (Invitrogen) supplemented with 0.5% Albumax I (Invitrogen), 25 mg l^{-1} hypoxanthine (Sigma), 10 mg l^{-1} gentamicin (Invitrogen) and 25 mM sodium bicarbonate (Sigma) using standard protocol described by Trager and Jensen (Trager and Jensen, 1976). *P. falciparum* 3D7 cultures were tightly synchronized by two rounds of successive sorbitol treatment as previously described (Lambros and Vanderberg, 1979). Progress of synchronized schizonts was periodically monitored by light microscopy of Giemsa stained smears. When majority of infected erythrocytes reached the mature schizont stage with segmented merozoites, the parasite culture was resuspended in buffer mimicking intracellular ionic conditions (IC buffer – 142 mM KCl, 5 mM NaCl, 2 mM EGTA, 1 mM $MgCl_2$, 5.6 mM glucose, 25 mM Hepes, pH 7.2). Schizonts were allowed to rupture and release merozoites over a period of 40 min. Cultures containing unruptured schizonts and released merozoites were centrifuged at 787 *g* in Eppendorf 5810R centrifuge for 5 min to separate released merozoites from unruptured schizonts and uninfected erythrocytes. Supernatant containing free merozoites was centrifuged at 3300 *g* using Eppendorf 5810R centrifuge for 5 min to collect merozoites as described previously (Singh *et al*., 2010). Merozoites were resuspended in IC buffer and used for experiments as described below.

Microneme secretion assay

Plasmodium falciparum merozoites in IC buffer were incubated with CN inhibitors FK506 (5 μM) and CsA (25 μM) or actin polymerization modulators, CytD (0.5–2 μM), ML-B (0.5–2 μM), LA-B (1–5 μM) and JAS (0.1–0.5 μM) for 15 min at 37°C and shifted to buffer mimicking extracellular ionic conditions (EC buffer – 5 mM

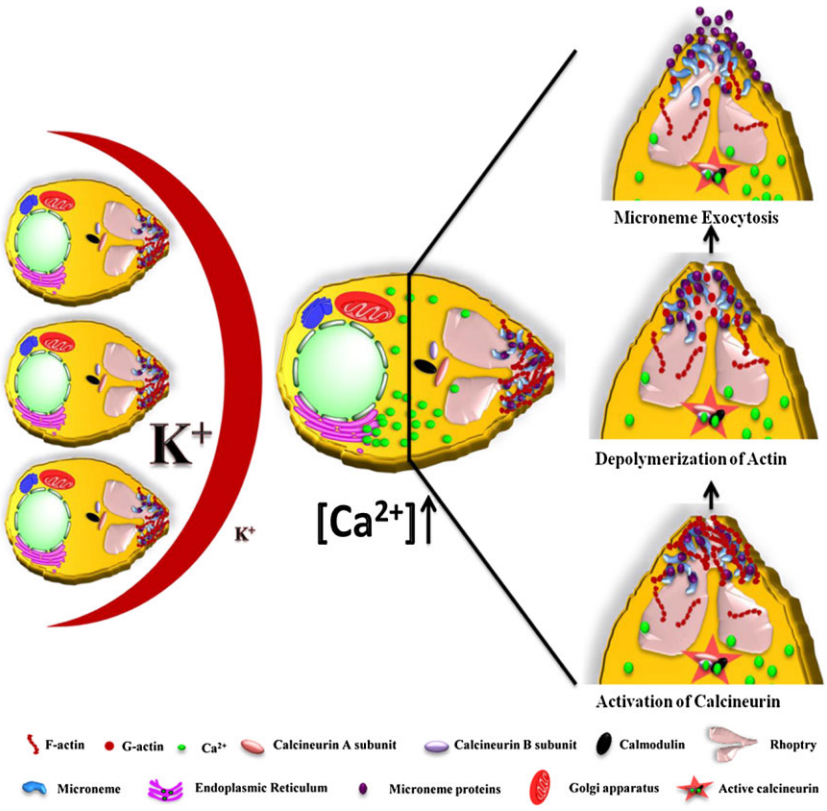

Fig. 7. Model summarizing putative role of CN and actin dynamics in microneme secretion in *P. falciparum* merozoites. Exposure of merozoites to a low K^+ environment stimulates rise in cytosolic Ca^{2+} that activates PfCN, which in turn leads to dephosphorylation of actin. Actin dephosphorylation stimulates depolymerization of F-actin, which reduces the physical barrier created by actin filaments and enables the docking of microneme to the apical plasma membrane and discharge of microneme proteins.

KCl, 142 mM NaCl, 1 mM $CaCl_2$, 1 mM $MgCl_2$, 5.6 mM glucose and 25 mM Hepes, pH 7.2) with CN inhibitors and actin modulators at similar concentrations. In control experiments merozoites were transferred from IC buffer to EC buffer without any CN inhibitors or actin modulators. Following incubation in EC buffer for 10 min at 37°C, merozoites and supernatants were separated by centrifugation at 3300 *g* at room temperature for 5 min. Supernatants were analysed by SDS-PAGE and transferred to nitrocellulose membrane for Western blotting. Microneme protein PfAMA1 was detected using anti-PfAMA1 rabbit sera at 1:2000 dilution. Rabbit sera against the cytoplasmic *P. falciparum* nucleosome assembly protein-large (NAPL) (Chandra *et al.*, 2005) was used at 1:2000 dilution to detect NAPL in merozoite pellets and supernatants to control for number of merozoites used and merozoite lysis under different conditions respectively. Following incubation of nitrocellulose blots with primary antisera for 1 h, the blots were incubated with horseradish peroxidase (HRP) conjugated anti-rabbit IgG goat antibodies (Sigma) at 1:2000 dilution for 1 h. Blots were then developed with ECL plus Western blotting detection system kit (GE Healthcare) following manufacturer's specifications. Developed X-ray films were scanned and bands analysed for intensity by ImageJ software.

Calcineurin activity assay

Plasmodium falciparum merozoites isolated in IC buffer as described above were incubated with CN inhibitors FK506 (5 μM) and CsA (25 μM) for 15 min at 37°C and transferred to EC buffer with the same inhibitors. Control merozoites were transferred from IC to EC buffer without any inhibitors. Merozoites in IC, EC, EC + FK506 (5 μM) and EC + CsA (25 μM) were lysed with lysis buffer (50 mM Tris, pH 7.5, 0.1 mM EDTA, 0.1 mM EGTA, 1 mM DTT, 0.2% NP-40). Merozoite lysates were centrifuged to remove cell debris. Excess phosphates and nucleotides were removed from the supernatants using a desalting column. Ca^{2+}-dependent phosphatase activity in merozoite lysates was measured as described by manufacturers of a CN activity measurement kit (ENZO, USA). Total phosphatase activity was assessed in the samples by incubating lysates with a phospho-peptide substrate RII, and measuring released free phosphate by Malachite green assay using BIOMOL GREEN reagent (Martin *et al.*, 1985). Ca^{2+}-independent phosphatase activity was assessed in the samples by incubating lysates with phosphopeptide substrate RII in presence of ethylene glycol tetra-acetic acid (EGTA). The Ca^{2+}-independent phosphatase activity was subtracted from total phosphatase activity to measure phosphatase activity attributable to PfCN.

Growth inhibition assay

Plasmodium falciparum merozoites isolated in IC buffer as described above were incubated with CN inhibitors FK506 (5 μM) and CsA (25 μM). Following incubation for 15 min with respective inhibitors, merozoites were resuspended in cRPMI containing erythrocytes at 2% haematocrit to allow invasion. After 24–26 h of incubation at 37°C under 5% CO_2, 5% O_2 and balanced with N_2 newly invaded rings were scored by light microscopy of Giemsa (Sigma, USA) stained smears. Per cent inhibition of invasion was calculated under each assay condition using the formula: $(1 - T/C) \times 100$; where T and C denote parasitaemia in treatment and control samples respectively.

Measurement of cytosolic Ca^{2+} by flow cytometry

Plasmodium falciparum merozoites isolated in complete RPMI or IC buffer as described above were loaded with 10 μM Fluo-4AM for 20 min at 37°C in IC buffer with or without inhibitors FK506 (5 μM) and CsA (25 μM). Fluo-4AM-loaded *P. falciparum* merozoites were transferred to EC buffer or EC buffer containing inhibitors FK506 (5 μM) and CsA (25 μM). Fluorescence signal from Fluo-4AM-labelled merozoites was analysed by flow cytometry on FACSCalibur (Becton Dickinson, USA) using CellQuest software. The Fluo-4AM-loaded merozoites were excited at 488 nm and fluorescence signal was detected with a 430/30 nm band pass filter for periods of 2–3 min. Merozoites were gated on the basis of their forward scatter and side scatter. Histograms of mean fluorescence intensity (MFI), which reflects cytosolic Ca^{2+} levels in merozoites, were plotted against time using FlowJo software.

Identification of phosphorylated proteins

Plasmodium falciparum merozoites isolated in IC buffer as described above were incubated with CN inhibitors FK506 (5 μM) and CsA (25 μM) for 15 min at 37°C and transferred to EC buffer with the same inhibitors. Control merozoites were transferred from IC to EC buffer without any inhibitors. Merozoites in IC, EC, EC + FK506 (5 μM) and EC + CsA (25 μM) buffers were pelleted and washed three times in PBS and resuspended in 10 volumes of ice-cold TNET buffer (50 mM Tris-HCl pH 8.0, 400 mM NaCl, 5 mM EDTA pH 8.0 and 0.5% Triton X-100) in presence of protease inhibitors cocktail (Roche Diagnostics). Parasites were lysed by freeze–thaw using liquid nitrogen. The extract was clarified by centrifugation at 13 000 *g* for 30 min at 4°C. Lysates were then boiled for 10 min, centrifuged to remove debris and the supernatant was separated on 12% SDS-PAGE. Phosphorylated proteins were visualized by staining SDS-PAGE gels with Pro-Q Diamond (Invitrogen, USA), a fluorescent dye that specifically binds phospho-amino acids. Stained gels were visualized with a Typhoon TM 9400 Variable Mode imager (GE Healthcare) with excitation at 532 nm and emission at 580 nm (± 30 nm).

The same gel was washed twice in dH_2O and re-stained overnight with a solution of SYPRO Ruby dye, which detects all proteins. The gel was washed two times for 30 min in destaining solution (10% methanol and 7% acetic acid), rinsed with dH_2O, scanned at 473 nm and emission signal was recorded at 610 nm. myImage Analysis (Thermo Scientific) software was used to measure the intensity of the Pro-Q Diamond and SYPRO Ruby signals for each band in each lane of the gel. This provided both pixel intensity and position information along the length of a lane. The median intensity values of the peaks corresponding to each band were used to calculate the fold changes in phosphorylated proteins following transfer of merozoites from one buffer condition to another. Signal from SYPRO Ruby stained gels was used to normalize the fold changes in phosphorylated proteins under different conditions.

Next, the SDS-PAGE gel was stained with Coomassie Brilliant Blue R-250 (Bio-Rad Laboratories) to visualize the bands with a visible permanent dye. Bands of interest were excised from the gel and subjected to identification by mass-spectrometry as follows.

Coomassie-stained gel pieces were washed twice with 100 mM NH_4HCO_3 (Sigma, USA) and 100% acetonitrile, reduced and alkylated using 25 mM DTT and 55 mM iodoacetamide, respectively, and incubated with 200 ng Trypsin Gold (Promega) in 25 mM NH_4HCO_3 for 3 h at 37°C. After digestion, samples were eluted from the gel with 50% acetonitrile, 2.5% tri-fluoro acetic acid and spotted onto a MALDI target and overlaid with 0.5 μl of 5 mg ml^{-1} MALDI matrix (α-cyano-4-hydroxycinnamic acid) (Sigma, USA) and 10 mM ammonium mono-basic phosphate (Sigma, USA). Mass spectrometric data were collected using an ABI 4800 MALDI TOF/TOF (Applied Biosystems, Foster City, CA). In most of the cases the data were acquired in reflector mode from a mass range of 600–4000 Daltons. Five most intense ions from the MS analysis, which are not on the exclusion list, were subjected to MS/MS with appropriate precursor mass range. GPS Explorer software (Applied Biosystems, Foster City, CA) was used to generate peak list from the raw data generated by the ABI 4800. The peak list was generated based on signal to noise filtering, exclusion list and de-isotoping parameters. The resulting peak list file was searched and compared against existing databases like Swissport and NCBI using Mascot (Matrix Science, Boston, MA). This experiment was performed two times. Proteins with significant scores (Mascot score > 67) identified from each excised protein band were ranked by their Mascot scores.

Immunoprecipitation (IP) of actin

Plasmodium falciparum merozoites isolated in IC buffer were incubated with CN inhibitors FK506 (5 μM) and CsA (25 μM) for 15 min at 37°C and transferred and incubated in EC buffer containing 40 μCi of [γ-^{32}P]-ATP (Perkin Elmer, USA) and the same inhibitors for 5 min at 37°C. Control merozoites were transferred from IC to EC buffer containing [γ-^{32}P]-ATP (Perkin Elmer, USA). Merozoites were collected by centrifugation and resuspended in 10 volumes of lysis/wash buffer (0.025 M Tris, 0.15 M NaCl, 0.001 M EDTA, 1% NP40, 5% glycerol; pH 7.4) supplied with Pierce Co-Immunoprecipitation (Co-Ip) Kit (Pierce, USA). Merozoites were lysed by three cycles of freeze thaw in liquid nitrogen followed by incubation at 37°C. Cell debris were removed by centrifugation at 13 000 *g* for 10 min at 4°C. Respective lysates were cleared with control agarose beads supplied with kit as per manufacturer protocol. Immunoprecipitation with anti-actin rabbit sera (Sigma-Aldrich) was performed as per manufacturer's protocol. Western blotting using anti-actin rabbit sera confirmed that equal amounts of actin were immunoprecipitated from merozoites under different conditions. Incorporation of ^{32}P in immunoprecipitated actin was detected using Storage Phosphor Screen (GE Healthcare). Phosphorylation of actin was quantified by densitometry using Typhoon TM 9400 Variable Mode imager (GE Healthcare).

Actin polymerization assay

Plasmodium falciparum merozoites isolated in IC buffer as described above were incubated with CN inhibitors FK506 (5 μM) and CsA (25 μM) and actin polymerization modulators CytD (2 μM) and JAS (0.5 μM) for 15 min at 37°C and transferred to EC buffer with the same inhibitors. Control merozoites were transferred from IC to EC buffer without any inhibitors. Following incubation in EC buffer for 10 min at 37°C, merozoites and supernatants were separated by centrifugation at 3300 *g* at room tem-

perature for 5 min and amount of G-actin/F-actin in merozoite lysates was estimated. Separation of *P. falciparum* F-actin from G-actin by ultracentrifugation of merozoite lysates and its detection by Western blotting has been described (Schmitz *et al*., 2010). We used an *in vivo* assay kit (Cytoskeleton, USA) for estimation of G-actin/F-actin. Treated merozoites were lysed with 10 volumes of lysis buffer (50 mM PIPES pH 6.9, 50 mM NaCl, 5 mM $MgCl_2$, 25 mM EGTA, 5% (v/v) glycerol, 0.1% Nonidet P40, 0.1% Triton X-100, 0.1% Tween 20, 0.1% 2-mercapto-ethanol, 0.001% Antifoam C) and centrifuged at 2000 r.p.m. for 5 min to pellet unbroken cells. The supernatant was subjected to ultracentrifugation for 1 h at 100 000 *g* using a desktop ultracentrifuge (Beckman Optima MAX, USA) to separate F-actin from soluble G-actin. Fractions containing F-actin (pellet) and G-actin (supernatant) were separated on SDS-PAGE gels and transferred to nitrocellulose membrane for Western blotting. Actin was detected with anti-actin rabbit sera (at 1:1000 dilution) raised against N-terminal 13-amino-acid peptide (GFAGDDAPRAVFP) of human actin (Sigma-Aldrich, USA). Among these 13 amino acids, 11 amino acids (GvAGDDAPRaVFP) are conserved in *P. falciparum* actin (Pfactin). Blots were then incubated with HRP-conjugated anti-rabbit IgG goat antibodies (Sigma) at 1:2000 dilution for 1 h. Blots were developed with ECL plus Western blotting detection system kit (GE Healthcare) following manufacturer's specifications. Developed X-ray films were scanned and intensity of bands was analysed by ImageJ software.

Immunofluorescence assay (IFA)

Plasmodium falciparum merozoites isolated in IC buffer as described above were incubated with or without CN inhibitors FK506 (5 μM) and CsA (25 μM) or actin polymerization modulators CytD (2 μM) and JAS (0.5 μM) for 15 min at 37°C and shifted to EC buffer with or without CN inhibitors and actin polymerization modulators. Thin smears of such merozoites were made on glass slides, air-dried and fixed in pre-chilled methanol for 20 min at −20°C. The slides were blocked with 3% BSA in PBS at room temperature for 1 h. Slides were incubated with anti-actin rabbit serum (1:500) and anti-PfEBA-175 mouse serum (1:500 dilution) OR Alexa Fluor 488-conjugated phalloidin and anti-PfEBA-175 mouse serum (1:500 dilution) followed by either Alexa Fluor 488-conjugated anti-rabbit IgG goat antibodies (1:500 dilution) (Molecular Probes) or Alexa Fluor 594-conjugated anti-mouse IgG goat serum (1:800) (Molecular Probes). Slides were mounted with ProLong Gold antifade reagent with 4′, 6-diamidino-2-phenylindole (DAPI) (Invitrogen) and analysed using a Nikon A1 confocal microscope. For clear visual assessments of localization, images were processed by Imaris version 6.4.2 or 7.0.0 (Bitplane Scientific), which provides functionality for visualization, segmentation and interpretation of 3D microscopy data sets. For clarity of display, deconvolved Z stacks were reconstructed in 3D, with interpolation.

Acknowledgements

This work was supported by MALSIG and EVIMaLaR grants from European Commission, Program Support grant to Malaria Group, ICGEB from Department of Biotechnology (DBT), Government of India and Indo-Swiss bilateral project grant from Department of Science and Technology (DST). C.C. is a recipient of the TATA Innovation Fellowship from DBT. S.S. is a recipient of an Innovative Young Biotechnologist Award (IYBA) from DBT. K.R.M. is recipient of Senior Research Fellowship of the Council of Scientific and Industrial Research (CSIR), Government of India.

References

Aunis, D., and Bader, M.F. (1988) The cytoskeleton as a barrier to exocytosis in secretory cells. *J Exp Biol* **139:** 253–266.

Baba, T., Fusaki, N., Shinya, N., Iwamatsu, A., and Hozumi, N. (2003) Actin tyrosine dephosphorylation by the Src homology 1-containing protein tyrosine phosphatase is essential for actin depolymerization after membrane IgM cross-linking. *J Immunol* **170:** 3762–3768.

Bansal, A., Singh, S., More, K.R., Hans, D., Nangalia, K., Yogavel, M., *et al*. (2013) Characterization of *Plasmodium falciparum* calcium-dependent protein kinase 1 (PfCDPK1) and its role in microneme secretion during erythrocyte invasion. *J Biol Chem* **288:** 1590–1602.

Carrero, J.C., Lugo, H., Pérez, D.G., Ortiz-Martínez, C., and Laclette, J.P. (2004) Cyclosporin A inhibits calcineurin (phosphatase 2B) and P-glycoprotein activity in *Entamoeba histolytica*. *Int J Parasitol* **34:** 1091–1097.

Carruthers, V.B., and Sibley, L.D. (1999) Mobilization of intracellular calcium stimulates microneme discharge in *Toxoplasma gondii*. *Mol Microbiol* **31:** 421–428.

Carruthers, V.B., Giddings, O.K., and Sibley, L.D. (1999) Secretion of micronemal proteins is associated with toxoplasma invasion of host cells. *Cell Microbiol* **1:** 225–236.

Chandra, B.R., Olivieri, A., Silvestrini, F., Alano, P., and Sharma, A. (2005) Biochemical characterization of the two nucleosome assembly proteins from *Plasmodium falciparum*. *Mol Biochem Parasitol* **142:** 237–247.

Cowman, A.F., and Crabb, B.S. (2006) Invasion of red blood cells by malaria parasites. *Cell* **124:** 755–766.

Dobson, S., May, T., Berriman, M., Vecchio, C.D., Fairlamb, A.H., Chakrabarti, D., and Barik, S. (1999) Characterization of protein Ser : Thr phosphatases of the malaria parasite, *Plasmodium falciparum*: inhibition of the parasitic calcineurin by cyclophilin–cyclosporin complex. *Mol Biochem Parasitol* **99:** 167–181.

Donella-Deana, A., Krinks, M.H., Ruzzene, M., Klee, C., and Pinna, L.A. (1994) Dephosphorylation of phosphopeptides by calcineurin (protein phosphatase 2B). *Eur J Biochem* **219:** 109–117.

Eitzen, G. (2003) Actin remodeling to facilitate membrane fusion. *Biochim Biophys Acta* **1641:** 175–181.

Enz, A., Shapiro, G., Chappuis, A., and Dattler, A. (1994) Nonradioactive assay for protein phosphatase 2B (Calcineurin) activity using a partial sequence of the subunit of cAMP-dependent protein kinase as substrate. *Anal Biochem* **216:** 147.

Farrell, A., Thirugnanam, S., Lorestani, A., Dvorin, J.D., Eidell, K.P., Ferguson, D.J.P., *et al*. (2012) A DOC2 Protein identified by mutational profiling is essential for apicomplexan parasite exocytosis. *Science* **335:** 218.

Gasman, S., Chasserot-Golaz, S., Malacombe, M., Way, M., and Bader, M.F. (2004) Regulated exocytosis in neuroendocrine cells: a role for subplasmalemmal Cdc42/

N-WASP-induced actin filaments. *Mol Biol Cell* **15:** 520–531.

Gaur, D., and Chitnis, C.E. (2011) Molecular interactions and signaling mechanisms during erythrocyte invasion by malaria parasites. *Curr Opin Microbiol* **14:** 422–428.

Goto, S., Yamamoto, H., Fukunaga, K., Iwasa, T., Matsukado, Y., and Miyamoto, E. (1985) Dephosphorylation of microtubule-associated protein 2, tau factor, and tubulin by calcineurin. *J Neurochem* **45:** 276–283.

Griffith, J.P., Kim, J.L., Kim, E.E., Sintchak, M.D., Thomson, J.A., Fitzgibbon, M.J., *et al*. (1995) X-ray structure of calcineurin inhibited by the immunophilin-immunosuppressant FKBP12–FK506 complex. *Cell* **82:** 507–522.

Grybko, M.J., Bartnik, J.P., Wurth, G.A., Pores-Fernando, A.T., and Zweifach, A. (2007) Calcineurin activation is only one calcium-dependent step in cytotoxic T lymphocyte granule exocytosis. *J Biol Chem* **282:** 18009–18017.

Hemenway, C.S., and Heitman, J. (1999) Calcineurin. Structure, function, and inhibition. *Cell Biochem Biophys* **30:** 115–151.

Ho, S., Clipstone, N., Timmermann, L., Northrop, J., Graef, I., Fiorentino, D., *et al*. (1996) The mechanism of action of cyclosporin A and FK506. *Clin Immunol Immunopathol* **80:** S40–S45.

Huai, Q., Kim, H.Y., Liu, Y., Zhao, Y., Mondragon, A., Liu, J.O., and Ke, H. (2002) Crystal structure of calcineurin–cyclophilin–cyclosporin shows common but distinct recognition of immunophilin–drug complexes. *Proc Natl Acad Sci USA* **99:** 12037–12042.

Johns, L.M., Levitan, E.S., Shelden, E.A., Holz, R.W., and Axelrod, D. (2001) Restriction of secretory granule motion near the plasma membrane of chromaffin cells. *J Cell Biol* **153:** 177–190.

Karch, C.M., Jeng, A.T., and Goate, A.M. (2013) Calcium phosphatase calcineurin influences tau metabolism. *Neurobiol Aging* **34:** 374–386.

Klee, C.B., Crouch, T.H., and Krinks, M.H. (1979) Calcineurin: a calcium- and calmodulin-binding protein of the nervous system. *Proc Natl Acad Sci USA* **76:** 6270–6273.

Kumar, R., Musiyenko, A., Oldenburg, A., Adams, B., and Barik, S. (2004) Post-translational generation of constitutively active cores from larger phosphatases in the malaria parasite, *Plasmodium falciparum*: implications for proteomics. *BMC Mol Biol* **5:** 6.

Kumar, R., Musiyenko, A., and Barik, S. (2005) *Plasmodium falciparum* calcineurin and its association with heat shock protein 90: mechanisms for the antimalarial activity of cyclosporin A and synergism with geldanamycin. *Mol Biochem Parasitol* **141:** 29–37.

Lambros, C., and Vanderberg, J.P. (1979) Synchronization of *Plasmodium falciparum* erythrocytic stages in culture. *J Parasitol* **65:** 418–420.

Lang, J. (1999) Molecular mechanisms and regulation of insulin exocytosis as a paradigm of endocrine secretion. *Eur J Biochem* **259:** 3–17.

Li, W., and Handschumacher, R.E. (2002) Identification of two calcineurin B-binding proteins: tubulin and heat shock protein 60. *Biochim Biophys Acta* **1599:** 72–81.

Liu, J., Farmer, J.D., Jr, Lane, W.S., Friedman, J., Weissman, I., and Schreiber, S.L. (1991) Calcineurin is a common target of cyclophilin-cyclosporin A and FKBP-FK506 complexes. *Cell* **66:** 807–815.

Lourido, S., Shuman, J., Zhang, C., Shokat, K.M., Hui, R., and Sibley, L.D. (2010) Calcium-dependent protein kinase 1 is an essential regulator of exocytosis in *Toxoplasma*. *Nature* **465:** 359–362.

Lovett, J.L., Marchesini, N., Moreno, S.N., and Sibley, L.D. (2002) *Toxoplasma gondii* microneme secretion involves intracellular Ca(2+) release from inositol 1,4,5-triphosphate (IP(3))/ryanodine-sensitive stores. *J Biol Chem* **277:** 25870–25876.

Martin, B., Pallen, C.J., Wang, J.H., and Graves, D.J. (1985) Use of fluorinated tyrosine phosphates to probe the substrate specificity of the low molecular weight phosphatase activity of calcineurin. *J Biol Chem* **260:** 14932–14937.

Momayezi, M., Lumpert, C.J., Kersken, H., Gras, U., Plattner, H., Krinks, M.H., and Klee, C.B. (1987) Exocytosis induction in *Paramecium tetraurelia* cells by exogenous phosphoprotein phosphatase *in vivo* and *in vitro*: possible involvement of calcineurin in exocytotic membrane fusion. *J Biol Chem* **105:** 181–189.

Muallem, S., Kwiatkowska, K., Xu, X., and Yin, H.L. (1995) Actin filament disassembly is a sufficient final trigger for exocytosis in nonexcitable cells. *J Cell Biol* **128:** 589–598.

Mukai, H., Kuno, T., Chang, C.-D., Lane, B., Luly, J.R., and Tanaka, C. (1993) FKBP12-FK506 complex inhibits phosphatase activity of two mammalian isoforms of calcineurin irrespective of their substrates or activation mechanisms. *J Biochem (Tokyo)* **113:** 292–298.

Murray, C.J., Rosenfeld, L.C., Lim, S.S., Andrews, K.G., Foreman, K.J., Haring, D., *et al*. (2012) Global malaria mortality between 1980 and 2010: a systematic analysis. *Lancet* **379:** 413–431.

Nickell, S.P., Scheibel, L.W., and Cole, G.A. (1982) Inhibition by cyclosporine A of rodent malaria *in vivo* and human malaria *in vitro*. *Infect Immun* **37:** 1093–1100.

O'Keefe, S.J., Tumura, J., Kincaid, R.L., Tocci, M.J., and O'Neill, E.A. (1992) FK-506- and CsA-sensitive activation of the interleukin-2 promoter by calcineurin. *Nature* **357:** 692–694.

Ohta, Y., Akiyama, T., Nishida, E., and Sakai, H. (1987) Protein kinase C and cAMP-dependent protein kinase induce opposite effects on actin polymerizability. *FEBS Lett* **222:** 305–310.

Pores-Fernando, A.T., Gaur, S., Doyon, M.Y., and Zweifach, A. (2009) Calcineurin dependent lytic granule exocytosis in NK-92 Natural Killer cells. *Cell Immunol* **254:** 105–109.

Saito, S., Watabe, S., Ozaki, H., Fusetani, N., and Karaki, H. (1994) Mycalolide B, a novel actin depolymerizing agent. *J Biol Chem* **269:** 29710–29714.

Schmitz, S., Schaap, I.A.T., Kleinjung, J., Harder, S., Grainger, M., Calder, L., *et al*. (2010) Malaria parasite actin polymerization and filament structure. *J Biol Chem* **285:** 36577–36585.

Schreiber, S.L., and Crabtree, G. (1993) The mechanism of action of cyclosporin A and FK506. *Immunol Today* **13:** 136–142.

Schulenberg, B., Aggeler, R., Beechem, J.M., Capaldi, R.A., and Patton, W.F. (2003) Analysis of steady-state protein

phosphorylation in mitochondria using a novel fluorescent phosphosensor dye. *J Biol Chem* **278:** 27251–27255.
Siddiqui, F.A., Dhawan, S., Singh, S., Singh, B., Gupta, P., Pandey, A., *et al*. (2013) Functional characterization of a thrombospondin structural repeat containing rhoptry protein from *Plasmodium falciparum* merozoites. *Cell Microbiol* **15:** 1341–1356.
Silverman-Gavrila, L.B., and Charlton, M.P. (2009) Calcineurin and cytoskeleton in low-frequency depression. *J Neurochem* **109:** 716–732.
Singh, S., Alam, M.M., Pal-Bhowmick, I., Brzostowski, J.A., and Chitnis, C.E. (2010) Distinct external signals trigger sequential release of apical organelles during erythrocyte invasion by malaria parasites. *PLoS Pathog* **6:** e1000746.
Spector, I., Braet, F., Shochet, N.R., and Bubb, M.R. (1999) New anti-actin drugs in the study of the organization and function of the actin cytoskeleton. *Microsc Res Tech* **47:** 18–37.
Su, F.F., Shi, M.Q., Guo, W.G., Liu, X.T., Wang, H.T., Lu, Z.F., and Zheng, Q.S. (2012) High-mobility group box 1 induces calcineurin-mediated cell hypertrophy in neonatal rat ventricular myocytes. *Mediators Inflamm* **2012:** 805149.
Swanson, S.K.-H., Born, T., Zydowsky, L.D., Cho, H., Chang, H.Y., Walsh, C.T., and Rusnak, F. (1992) Cyclosporin-mediated inhibition of bovine calcineurin by cyclophilins A and B. *Proc Natl Acad Sci USA* **89:** 3741–3745.
Thommen-Scott, K. (1981) Antimalarial activity of cyclosporine A. *Agents Actions* **11:** 770–773.
Tobin, V., Leng, G., and Ludwig, M. (2012) The involvement of actin, calcium channels and exocytosis proteins in somato-dendritic oxytocin and vasopressin release. *Front Physiol* **3:** article 261.
Trager, W., and Jensen, J.B. (1976) Human malaria parasites in continuous culture. *Science* **193:** 673–675.
Treeck, M., Sanders, J.L., Elias, J.E., and Boothroyd, J.C. (2011) The phosphoproteomes of *Plasmodium falciparum* and *Toxoplasma gondii* reveal unusual adaptations within and beyond the parasites' boundaries. *Cell Host Microbe* **10:** 410–419.
Tu, Y., Wu, S., Shi, X., Chen, K., and Wu, C. (2003) Migfilin and Mig-2 link focal adhesions to filamin and the actin cytoskeleton and function in cell shape modulation. *Cell* **113:** 37–47.
Vitale, M.L., Rodriguez Del Castillo, A., Tchakarov, L., and TrifarÓ, J.-M. (1991) Cortical filamentous actin disassembly and Scinderin redistribution during Chromatfin cell stimulation precede exocytosis, a phenomenon not exhibited by Gelsolin. *J Cell Biol* **113:** 1057–1067.
Webb, S.E., Fowler, R.E., O'shaughnessy, C., Pinder, J.-C., Dluzewski, A.R., Gratzer, W.B., *et al*. (1996) Contractile protein system in the asexual stages of the malaria parasite *Plasmodium falciparum*. *Parasitology* **112:** 451–457.
Wiederrecht, G., Lam, E., Hung, S., Martin, M., and Sigal, N. (1993) The mechanism of action of FK-506 and cyclosporin A. *Ann N Y Acad Sci* **696:** 9–19.
Yoneda, M., Nishizaki, T., Tasaka, K., Kurachi, H., Miyake, A., and Murata, Y. (2000) Changes in actin network during calcium-induced exocytosis in permeabilized GH3 cells: calcium directly regulates F-actin disassembly. *J Endocrinol* **166:** 677–687.

Supporting information

Additional Supporting Information may be found in the online version of this article at the publisher's web-site:

Fig. S1. Quantitative analysis of polymerization status of actin in *P. falciparum* merozoites. Densitometric scan analyses were performed on confocal images of Alexa 488-phalloidin-stained merozoites treated with IC, EC, EC + 5 μM FK506, EC + 25 μM CsA, EC + 2 μM CytD and EC + 0.5 μM JAS. A region of interest (ROI) was drawn to include the complete merozoite and mean fluorescence intensity (MFI) was calculated. The average MFI for the ROI determined for 50 merozoites under each experimental condition are plotted.
Fig. S2. Effect of actin modulators on *in vivo* CN activity in *P. falciparum* merozoites. Activity of PfCN was assessed in *P. falciparum* merozoites in IC buffer or after transfer to EC buffer with or without treatment with CytD (2 μM), JAS (0.5 μM), LA-B (5 μM) or ML-B (2 μM) using CN cellular activity assay kit (Enzo Life Sciences, USA). Transfer of merozoites from IC to EC buffer triggers PfCN activity. Treatment of merozoites with actin modulators CytD, JAS, LA-B or ML-B has no effect on PfCN activity. Error bars represent standard deviations from three independent experiments.
Fig. S3. Effect of actin modulators on invasion of P. falciparum merozoites. *P. falciparum* merozoites were pre-treated with CytD (2 μM), JAS (0.5 μM), LA-B (5 μM) or ML-B (2 μM) in IC buffer and added to erythrocytes resuspended in RPMI to allow invasion. Newly invaded rings were scored by Giemsa staining 24–26 h post invasion. Per cent (%) inhibition of invasion by different actin modulators is shown. Error bars represent standard deviations determined from three independent experiments.
Table S1. List of proteins identified by mass spectrometry. Proteins identified by mass spectrometry with significant Mascot score (score > 67) were listed. For each band, proteins identified from two independent experiments were listed. Proteins with highest cumulative Mascot score are represented in bold.